

# Relative effectiveness of weak periodic excitations in suppressing homoclinic/heteroclinic chaos

R. Chacón<sup>a</sup>

Departamento de Electrónica e Ingeniería Electromecánica, Escuela de Ingenierías Industriales, Universidad de Extremadura, 06071 Badajoz, Spain

Received 21 May 2002 / Received in final form 13 September 2002

Published online 29 November 2002 – © EDP Sciences, Società Italiana di Fisica, Springer-Verlag 2002

**Abstract.** Melnikov-method-based theoretical results are demonstrated concerning the *relative* effectiveness of *any* two weak excitations in suppressing homoclinic/heteroclinic chaos of a relevant class of dissipative, low-dimensional and non-autonomous systems for the main resonance between the chaos-inducing and chaos-suppressing excitations. General analytical expressions are derived from the analysis of generic Melnikov functions providing the boundaries of the regions as well as the enclosed area in the amplitude/initial phase plane of the chaos-suppressing excitation where homoclinic/heteroclinic chaos is inhibited. The relevance of the theoretical results on chaotic attractor elimination is confirmed by means of Lyapunov exponent calculations for a two-well Duffing oscillator.

**PACS.** 05.45.Ac Low-dimensional chaos – 05.45.Pq Numerical simulations of chaotic models – 05.45.Gg Control of chaos, applications of chaos

Previous theoretical work [1–3] on chaos suppression in low-dimensional systems capable of being studied by the Melnikov method (MM) [4–7] by adding a small external harmonic excitation or by perturbing a system parameter with weak harmonic excitations is established in terms of theorems concerning the analysis of the simple zeros of generic Melnikov functions (MFs). For the case of subharmonic resonances between the two driving frequencies involved,  $\Omega = p\omega$  ( $\Omega(\omega)$  being the chaos-suppressing (chaos-inducing) frequency and  $p$  an integer), such theorems give necessary and sufficient conditions for the frustration of homoclinic/heteroclinic bifurcations, which is typically the underlying mechanism to the suppression of chaos in the aforementioned systems. In particular, these theorems provide analytical estimates for the intervals of initial phase difference  $\Theta$  between the two excitations involved on the one hand, and analytical estimates for the intervals of the chaos-suppressing amplitude  $\eta$  on the other, for which homoclinic/heteroclinic bifurcations can be inhibited. With regard to the theoretically predicted intervals of suppressory amplitudes, a weakness of the theoretical approach is that the upper amplitude threshold  $\eta_{\max}$  typically underestimates (unlike the lower amplitude threshold  $\eta_{\min}$ ) the corresponding upper threshold observed numerically. Clearly, one would also wish to have analytical functions  $\eta = \eta(\Theta)$  for the regularization (in the aforementioned sense) boundaries in the  $\Theta - \eta$  parameter plane, instead of separate sets of estimates for the (ranges of) suitable values of  $\eta$  and  $\Theta$ , respectively. An-

other point is that the aforementioned suppression theorems indistinctly deal with parametric and external excitations (such as chaos-inducing and chaos-suppressing excitations) although, to the best of the author's knowledge, a general discussion of the relative effectiveness of *any two* of such chaos-suppressing excitations has as of now not been undertaken, the only precedent being the specific problem of suppressing chaotic escape from a one-well Duffing oscillator by means of two particular chaos-suppressing excitations [8].

In this present work, generic functions  $\eta = \eta(\Theta)$  providing the regularization boundaries in the  $\Theta - \eta$  parameter plane are derived on the basis of MM for the *main* resonance case  $\Omega = \omega$ . Remarkably, such boundary functions yield more accurate upper amplitude thresholds than those predicted from the suppression theorems, and permit one to reliably determine the relative suppressory effectiveness – in the sense of the extension in the  $\Theta - \eta$  parameter plane – of generic parametric and external excitations. The pertinence of the theoretical findings to the elimination of chaotic attractors is illustrated with the example of a two-well Duffing oscillator.

The wide and relevant class of dissipative non-autonomous systems, described by the differential equations

$$\begin{aligned} \dot{x} &= v, \\ \dot{v} &= -\frac{dV(x)}{dx} - d(x, v) + h_c(x, v)F_c(t) + h_s(x, v)F_s(t), \end{aligned} \quad (1)$$

<sup>a</sup> e-mail: rchacon@unex.es

is studied, where  $V(x)$  is a general potential,  $-d(x, v)$  is a generic dissipative force,  $h_c(x, v)F_c(t)$  is a general temporal chaos-inducing excitation, and  $h_s(x, v)F_s(t)$  is an as yet undetermined suitable chaos-suppressing excitation, with  $F_c(t)$ ,  $F_s(t)$  being harmonic functions of common frequency  $\omega$  and initial phases  $0$ ,  $\Theta$ , respectively. It is also assumed that the complete system (1) satisfies the MM requirements, *i.e.*, the dissipation and excitation terms are small-amplitude perturbations of the underlying conservative system  $\dot{x} = v$ ,  $\dot{v} + dV(x)/dx = 0$  which has a separatrix (see [4–7] for a general background).

The application of MM to equation (1) yields the MF

$$M_{h,h'}^{\pm}(t_0) = D \pm Ahar(\omega t_0) + Bhar'(\omega t_0 + \varphi_{h,h'}^{\pm}), \quad (2)$$

where the notation  $har(x)$  means indistinctly  $\sin(x)$  or  $\cos(x)$ , and  $A$  is a non-negative function while  $D$ ,  $B$  can be negative or non-negative functions depending upon the respective parameters for each specific system. In particular,  $D$  contains the effect of the damping and constant drivings. In the absence of any constant driving,  $D < 0$ , while one has the three cases  $D \geq 0$  when a (positive) constant driving acts on the system besides the dissipative force. Also,  $A$  and  $B$  contain the effect of the chaos-inducing and chaos-suppressing excitations, respectively. Note that changing the sign of  $B$  is equivalent to having a fixed shift of the initial phase:  $B \rightarrow -B \iff \varphi_{h,h'}^{\pm} \rightarrow \varphi_{h,h'}^{\pm} \pm \pi$  where the two signs before  $\pi$  apply to each of the sign superscripts of  $\varphi$ . Therefore,  $B$  will be considered (for instance) to be a positive function in the following.

It is well known that the simple zeros of the MF give rise to transversal homoclinic points and chaotic phenomena [6]. Observe that, as initial time  $t_0$  and phase are not fixed, one can study the simple zeros of  $M_{h,h'}^{\pm}(t_0)$  by choosing quite freely the trigonometric functions in equation (2). Therefore, to illustrate the general procedure one can consider, for instance, the damped driven two-well Duffing oscillator [9–12], subjected to a PE of the cubic term, studied in [13]:

$$\ddot{x} - x + \beta x^3 = -\delta \dot{x} + \gamma \cos(\omega t) - \eta \beta x^3 \cos(\omega t + \Theta), \quad (3)$$

where  $\eta$  and  $\Theta$  are the normalized amplitude and initial phase, respectively, of the suppressory PE ( $0 < \delta$ ,  $\gamma$ ,  $\eta \ll 1$ ). The MF associated with the left homoclinic orbit is

$$M^-(\tau_0) = -D - A \sin(\omega \tau_0) - B \sin(\omega \tau_0 + \Theta), \quad (4)$$

with

$$\begin{aligned} D &\equiv \frac{4\delta}{3\beta}, \\ A &\equiv \left(\frac{2}{\beta}\right)^{1/2} \pi \gamma \omega \operatorname{sech}\left(\frac{\pi\omega}{2}\right), \\ B &\equiv \frac{\pi\eta}{6\beta} (4\omega^2 + \omega^4) \operatorname{csch}\left(\frac{\pi\omega}{2}\right). \end{aligned} \quad (5)$$

The MF (4) will be used to illustrate the generic method. Note that the MFs (2) and (4) are connected by linear relationships which are known for each specific system (1):

$$t_0 = t_0(\tau_0, \omega), \quad \Theta = \Theta(\varphi_{h,h'}^{\pm}). \quad (6)$$

Let us suppose that, in the absence of any chaos-suppressing excitation ( $B = 0$ ), the associated MF  $M_0^-(\tau_0) = -D - A \sin(\omega \tau_0)$  changes sign at some  $\tau_0$ , *i.e.*,  $D \leq A$ . Clearly, equation (4) can be recast into the form

$$\begin{aligned} M^-(\tau_0) &= -D - (A + B \cos \Theta) \sin(\omega \tau_0) \\ &\quad - B \sin \Theta \cos(\omega \tau_0) \\ &\leq -D + [(A + B \cos \Theta)^2 + B^2 \sin^2 \Theta]^{1/2}. \end{aligned} \quad (7)$$

If we now let the chaos-suppressing excitation act on the system such that

$$B^2 + 2AB \cos \Theta + A^2 - D^2 \leq 0, \quad (8)$$

this relationship represents a sufficient condition for  $M^-(\tau_0)$  to be negative (or null) for all  $\tau_0$ . The equals sign in equation (8) yields the boundary of the region in the  $\Theta - \eta$  plane where homoclinic chaos is suppressed:

$$\eta = \eta_{\sin, \sin}^- \equiv \left[ -\cos \Theta \pm \sqrt{\cos^2 \Theta - (1 - D^2/A^2)} \right] R, \quad (9)$$

with

$$R = R_{PE} \equiv \frac{6\sqrt{2}\beta\gamma}{4\omega + \omega^3} \tanh\left(\frac{\pi\omega}{2}\right) \quad (10)$$

(*cf.* Eqs. (5) and (8)), and where the sign  $+$  ( $-$ ) before the square root corresponds to the upper (lower) branch of the boundary. It is worth mentioning that a similar relationship to that in equation (8) is discussed in [14] for the particular case  $A = B$ , which is associated with a Duffing-van der Pol oscillator where the chaos-suppressing excitation is an additional forcing term with an initial phase  $\omega\varphi$  instead of  $\varphi$ . Similarly, the boundary functions corresponding to the respective MFs (2) are

$$\eta_{\cos, \cos}^{\pm} = \eta_{\sin, \sin}^{\pm} \equiv \left[ \mp \cos \varphi \pm \sqrt{\cos^2 \varphi - (1 - D^2/A^2)} \right] R, \quad (11a)$$

$$\eta_{\cos, \sin}^{\pm} = -\eta_{\sin, \cos}^{\pm} \equiv \left[ \mp \sin \varphi \pm \sqrt{\sin^2 \varphi - (1 - D^2/A^2)} \right] R, \quad (11b)$$

for  $B > 0$  (*cf.* Eq. (2)), and

$$\eta_{\cos, \cos}^{\pm} = \eta_{\sin, \sin}^{\pm} \equiv \left[ \pm \cos \varphi \pm \sqrt{\cos^2 \varphi - (1 - D^2/A^2)} \right] R, \quad (12a)$$

$$\eta_{\cos, \sin}^{\pm} = -\eta_{\sin, \cos}^{\pm} \equiv \left[ \pm \sin \varphi \pm \sqrt{\sin^2 \varphi - (1 - D^2/A^2)} \right] R, \quad (12b)$$

for  $B < 0$  (*cf.* Eq. (2)). The two signs before the square root apply to each of the sign superscripts of  $\eta_{h,h'}^{\pm}$ , which, in its turn, is *independent* of the sign of  $D$ .

### Remarks

First, the boundary functions (11, 12) represent loops in the  $\varphi - \eta$  plane which are symmetric with respect to the corresponding optimal suppressory value  $\varphi_{opt}$  predicted by the previous theoretical approach [1], as expected.

Second, the lower branch of each boundary functions (11, 12),  $\eta_{lower} = \eta_{lower}(\varphi)$ , exhibits a minimum at the corresponding  $\varphi_{opt}$  value, which is  $\eta = \eta_{min} \equiv (1 - |D|/A)R$ , *i.e.*, the lower amplitude threshold predicted by the suppression theorems [1].

Third, the maximum range of suppressory initial phase differences occurs when the upper and lower branches of the boundary functions coincide, *i.e.*, when the square root cancels out (*cf.* Eqs. (11, 12)). If  $\Delta\varphi_{max}$  denotes the maximum deviation from  $\varphi_{opt}$ , then, by substituting  $\varphi = \varphi_{opt} \pm \Delta\varphi_{max}$  into the square root and taking into account the respective value  $\varphi_{opt}$  for each MF  $M_{h,h'}^{\pm}$  (*cf.* [1]), one obtains  $\Delta\varphi_{max} = \arcsin(|D|/A)$  for all the cases, *i.e.*, one recovers the expression derived from the previous theoretical approach [1].

Fourth, the upper branch of each boundary functions (11, 12),  $\eta_{upper} = \eta_{upper}(\varphi)$ , exhibits a maximum at the respective  $\varphi_{opt}$  value, which is  $\eta = \eta_{max}^* \equiv (1 + |D|/A)R > \eta_{max} \equiv R$ , with  $\eta_{max}$  being the upper amplitude threshold predicted by the suppression theorems [1]. Computer simulations indicate that  $\eta_{max}^*$  is clearly closer than  $\eta_{max}$  to the respective numerically obtained threshold.

Fifth, the boundary functions (11, 12) permit one to reliably compare the relative effectiveness of *any two* chaos-suppressing excitations, in particular, external and parametric excitations. Indeed, since the functions  $A$ ,  $D$  are *fixed* for a given initial chaotic state ( $B = 0$ ), and the area enclosed by *any* boundary functions (11, 12) is given by

$$A_R \equiv \int_{\varphi_{opt} - \Delta\varphi_{max}}^{\varphi_{opt} + \Delta\varphi_{max}} (\eta_{upper} - \eta_{lower}) d\varphi = 4 \left( \frac{|D|}{A} \right) R, \quad (13)$$

the relative inhibitory effectiveness of any two chaos-suppressing excitations, denoted as I, II, can be quantified by

$$\frac{A_{R_I}}{A_{R_{II}}} = \frac{R_I}{R_{II}}. \quad (14)$$

Note that one finds  $A_R \rightarrow 0$  as  $D \rightarrow 0$ , as expected, which corresponds to the limiting Hamiltonian case with no constant drivings. Figure 1 summarizes the aforementioned properties of a generic boundary functions (11, 12). As an illustrative example of the area criterion, consider the damped driven two-well Duffing oscillator, subjected now to an additional forcing term, instead of a PE of the cubic term (*cf.* Eq. (3)):

$$\ddot{x} - x + \beta x^3 = -\delta \dot{x} + \gamma \cos(\omega t) + \eta \gamma \cos(\omega t + \Theta). \quad (15)$$

The MF associated with the left homoclinic orbit is

$$M'^-(\tau_0) = -D - A \sin(\omega\tau_0) - B' \sin(\omega\tau_0 + \Theta), \quad (16)$$

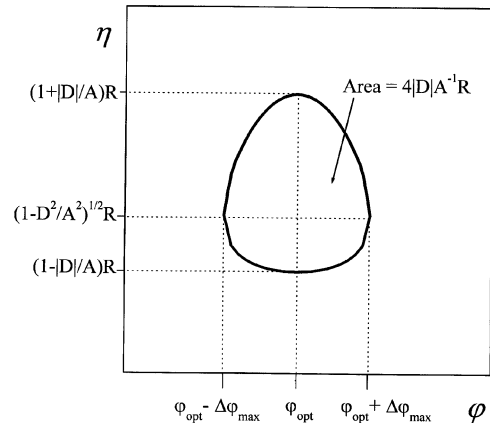


**Fig. 1.** Generic boundary function (*cf.* Eqs. (11, 12)) encircling the region where homoclinic/heteroclinic bifurcations are frustrated in the suppressory  $\varphi - \eta$  parameter plane.

with

$$B' = \left( \frac{2}{\beta} \right)^{1/2} \pi \eta \gamma \omega \operatorname{sech} \left( \frac{\pi \omega}{2} \right), \quad (17)$$

and  $D$ ,  $A$  given by equation (5). The corresponding boundary function is given by equation (9) (as in the PE case) now with

$$R = R_{AF} \equiv 1. \quad (18)$$

Thus, the area criterion (14) yields

$$\frac{A_{R_{PE}}}{A_{R_{AF}}} = \frac{6\sqrt{2}\beta\gamma}{4\omega + \omega^3} \tanh \left( \frac{\pi\omega}{2} \right), \quad (19)$$

whose value is one-to-one determined for each initial chaotic state. Generally, this means that the choice of the most suitable chaos-suppressing excitation can strongly depend upon the specific initial chaotic state to be considered.

Next, one can compare the theoretical results obtained from MM and Lyapunov exponent (LE) calculations of the two-well Duffing oscillator subjected to the two aforementioned types of chaos-suppressing excitations (*cf.* Eqs. (3) and (15)). It is worth noting that one cannot expect too good a quantitative agreement between the two kinds of findings because LE provides information concerning solely steady responses, while MM is a perturbative method generally related to transient chaos. LEs were computed using a version of the algorithm introduced in [15] and the integration was typically up to 2000 drive cycles for the fixed parameters  $\beta = 4$ ,  $\delta = 0.154$ ,  $\gamma = 0.095$ ,  $\omega = 1.1$ . In the absence of the chaos-suppressing excitations ( $\eta = 0$ ), the Duffing oscillator exhibits a strange chaotic attractor with a maximal LE  $\lambda^+(\eta = 0) = 0.127$  bits/s. The maximal LE was calculated for each point on an  $100 \times 100$  grid, with (normalized) initial phase  $\Theta$  and amplitude  $\eta$  along the horizontal and vertical axes, respectively, for both types of chaos-suppressing excitations. The results

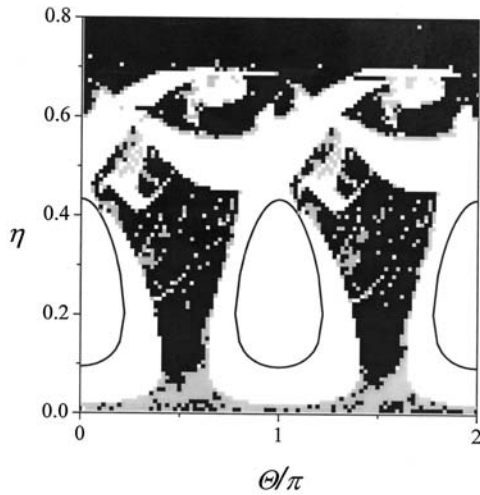


**Fig. 2.** Grid of  $100 \times 100$  points in the  $\Theta - \eta$  parameter plane for the two-well Duffing oscillator subjected to a chaos-suppressing PE (cf. Eq. (3)). Grey (black) squares indicate that the respective maximal LE,  $\lambda^+(\eta \neq 0)$ , is larger than  $10^{-3}$  ( $0.127 = \lambda^+(\eta = 0)$ ). Solid black contours indicate the two predicted boundary functions which are symmetric with respect to the optimal suppressory values  $0, \pi$ , respectively.

for the parametric and external chaos-suppressing excitations (cf. Eqs. (3) and (15), respectively) are shown in Figures 2 and 3, respectively. The diagrams in these figures were constructed by only plotting points on the grid when the respective LE was larger than  $10^{-3}$  (grey squares) or than  $\lambda^+(\eta = 0)$  (black squares), and with solid black contours denoting the respective theoretical boundary functions (cf. Eqs. (11a) and (12a)). One sees that complete regularization ( $\lambda^+(\eta \neq 0) \leq 0$ ) mainly appears inside maximal islands which *symmetrically* contain the respective theoretically predicted areas where even the chaotic transients are eliminated. The size of the main regularization islands is notably larger for the additional forcing case than for the PE case, which is in agreement with the area criterion:  $A_{RPE}/A_{RAF} \simeq 0.264097$  (cf. Eq. (19)). The structure of the secondary and minor islands of regularization is clearly more complex for the parametric than for the external chaos-suppressing excitation, as can be appreciated by comparison of Figures 2 and 3. Another difference is that the entire diagram of Figure 2 is periodic along the  $\Theta$ -axis, with fundamental period equal to  $\pi$  (note that there exist two optimal suppressory values  $\Theta_{opt,1} \equiv 0, \Theta_{opt,2} \equiv \pi$  (cf. [2])), while the entire diagram corresponding to the external excitation (Fig. 3) is symmetric with respect to the (single) optimal suppressory value  $\Theta_{opt} \equiv \pi$ . This is a consequence of the survival of the symmetries existing in the absence of chaos-suppressing excitations [2].

In summary, an MM-based theoretical approach has been presented concerning the relative effectiveness of weak periodic excitations in suppressing homoclinic/heteroclinic chaos of an important class of dissipative, low-dimensional and non-autonomous systems for the main resonance between the chaos-inducing and chaos-

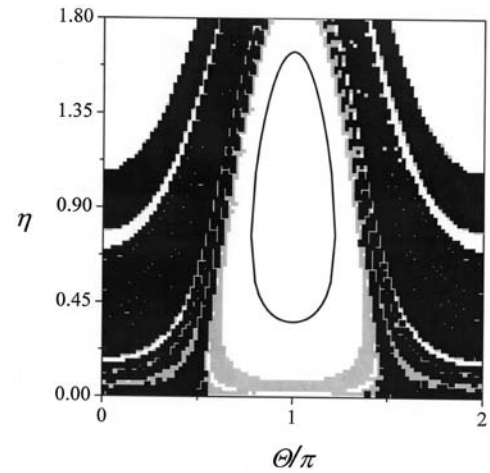


**Fig. 3.** Grid of  $100 \times 100$  points in the  $\Theta - \eta$  parameter plane for the two-well Duffing oscillator subjected to an external chaos-suppressing excitation (cf. Eq. (15)). Grey (black) squares indicate that the respective maximal LE,  $\lambda^+(\eta \neq 0)$ , is larger than  $10^{-3}$  ( $0.127 = \lambda^+(\eta = 0)$ ). The solid black contour indicates the predicted boundary function which is symmetric with respect to the single optimal suppressory value  $\pi$ .

suppressing excitations. A criterion based on the area in the suppressory amplitude/initial phase parameter plane, where suppression of homoclinic chaos is guaranteed, was deduced and shown to be useful in choosing the most suitable of the possible chaos-suppressing excitations. Additionally, the choice of the most suitable chaos-suppressing excitation was shown to exhibit sensitivity to the particular initial chaotic state.

The author thanks Prof. S. Rajasekar for kindly providing a reprint of [14], which was the origin of the present work. Partial financial support was provided by DGI (Spain) Grant No. BFM2002-00010.

## References

1. R. Chacón, Phys. Lett. A **257**, 293 (1999)
2. R. Chacón, Phys. Rev. Lett. **86**, 1737 (2001)
3. R. Chacón, Europhys. Lett. **54**, 148 (2001)
4. V.K. Melnikov, Trans. Moscow Math. Soc. **12**, 1 (1963)
5. V.I. Arnold, Sov. Math. Dokl. **5**, 581 (1964)
6. J. Guckenheimer, P.J. Holmes, *Nonlinear Oscillations, Dynamical Systems, and Bifurcations of Vector Fields* (Springer, 1983)
7. S. Wiggins, *Global Bifurcations and Chaos* (Springer-Verlag, 1988)
8. R. Chacón, Phys. Lett. A **249**, 431 (1998)
9. K. Wiesenfeld, B. McNamara, Phys. Rev. A **33**, 629 (1986)
10. P. Bryant, K. Wiesenfeld, Phys. Rev. A **33**, 2525 (1986)
11. L. Fronzoni, M. Giocondo, M. Pettini, Phys. Rev. A **43**, 6483 (1991)
12. J. Brindley, T. Kapitaniak, Chaos, Solitons Fractals **1**, 323 (1991)
13. R. Chacón, Phys. Rev. E **51**, 761 (1995)
14. S. Rajasekar, Pramana J. Phys. **41**, 295 (1993)
15. G. Benettin, L. Galgani, J.M. Strelcyn, Phys. Rev. A **14**, 2338 (1976)